ACCOUNTS of chemical research

Article

Cite This: Acc. Chem. Res. 2019, 52, 1824−1833

pubs.acs.org/accounts

Fullerenes as Nanocontainers That Stabilize Unique Actinide Species Inside: Structures, Formation, and Reactivity

Published as part of the Accounts of Chemical Research special issue "Advanced Molecular Nanocarbons".

Wenting Cai,[†,‡] Chia-Hsiang Chen,[∥,‡] Ning Chen,[*,§] and Luis Echegoyen[*,†]

[†]Department of Chemistry, University of Texas at El Paso, El Paso, Texas 79968, United States

[∥]Department of Medicinal and Applied Chemistry, Kaohsiung Medical University, Kaohsiung 807, Taiwan

[§]College of Chemistry, Chemical Engineering and Materials Science, Soochow University, Suzhou, Jiangsu 215123, P. R. China

CONSPECTUS: Fullerene carbon cages can encapsulate a wide variety of atoms, ions, clusters, or small molecules inside, resulting in stable compounds with unusual structures and electronic properties. These compounds are collectively defined as endohedral fullerenes. The most studied endohedral fullerenes are those containing metal atoms or ions inside, and these are referred to as endohedral metallofullerenes (EMFs). For EMFs, the inner isolated space of the fullerene cages can lead to the stabilization of unique clusters, which are otherwise not synthetically accessible. This offers an excellent environment and opportunity for investigating the nature of previously unobserved metal−metal, metal−non-metal, and metal−fullerene interactions, which are of fundamental interest and importance. Up until now, most of the work in this field has been mainly focused on the rare-earth metals and related elements (groups II, III, and IV). The encapsulation of other elements of the periodic table could potentially lead to totally new structures and bonding motifs and to material properties beyond those of the existing EMFs. Actinides were originally explored as encapsulated elements in fullerenes when Smalley et al. (*Science* **1992**, *257*, 1661) reported mass spectral evidence of actinide endohedral fullerenes back in 1992. However, the full characterization of these actinide endohedral fullerenes, including single crystal X-ray diffractometric analyses, was not reported until very recently, in 2017.

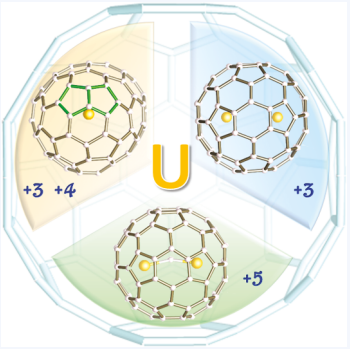

In this Account, we highlight some recent advances made in the field of EMF compounds, focusing primarily on the molecular and electronic structures of novel actinide-based EMFs, new evidence for the formation mechanisms of EMFs, and the influence of the entrapped species on the reactivity and regiochemistry of EMF compounds. We recently reported that some monometallic actinide EMFs represent the first examples of tetravalent metals encapsulated inside fullerenes that exhibit considerably stronger host−guest interactions when compared to those observed for the lanthanide EMFs. These unusually strong metal−cage interactions, along with very high mobilities of the actinides inside the fullerene cages at high temperatures, result in the stabilization of unexpected non-IPR (isolated pentagon rule) fullerene cages encapsulating only one metal ion. Strikingly, such covalent stabilization factors had never been previously observed, although Sm@C_{2v}(19138)-C_{76} was the first reported mono-EMF with a non-IPR cage, see details below. In addition, we showed that a long sought-after actinide−actinide bond was obtained upon encapsulation of U_2 inside an I_h(7)-C_{80} fullerene cage. More interestingly, we demonstrated that actinide multiple bonds, which are very difficult to prepare by conventional synthetic methods, are stabilized when trapped inside fullerene cages. A totally unexpected and previously unreported uranium carbide cluster, U═C═U, was fully characterized inside an EMF, U_2C@I_h(7)-C_{80}, which, for the first time, clearly exhibits two unsupported axial U═C double bonds that are ∼2.03 Å long. We also discovered that synthetic bis-porphyrin nanocapsules exhibit exquisitely selective complexation of some of these uranium endohedral compounds, providing the basis for a nonchromatographic EMF purification method for actinide EMFs. Regarding EMF formation mechanisms, we suggested that novel carbide EMF structures, that is, Sc_2C_2@C_s(hept)-C_{88}, are likely key intermediates in a bottom-up fullerene growth process. Additionally, the structural correlation between chiral carbon cages during a bottom-up growth process was shown to be enantiomer-dependent. The influence of the encapsulated clusters on the chemical reactivity of EMFs is discussed at the end, which showed that the regioselectivities of multiple additions to the fullerene cages are remarkably controlled by the encapsulated metal clusters.

1. INTRODUCTION

The first endohedral fullerene, La@C_{82}, was discovered by Smalley and co-workers in 1985,[1] thus marking the beginning of this unique and interesting research field. But it was not until 1990 that the study of the molecular structures, physiochemical properties, and reactivity of endohedral fullerenes became possible when the macroscopic-scale production of fullerenes was accomplished.[2] In 1999, Dorn and co-workers discovered the first cluster endohedral

Received: May 1, 2019
Published: July 1, 2019

DOI: 10.1021/acs.accounts.9b00229
Acc. Chem. Res. 2019, 52, 1824−1833

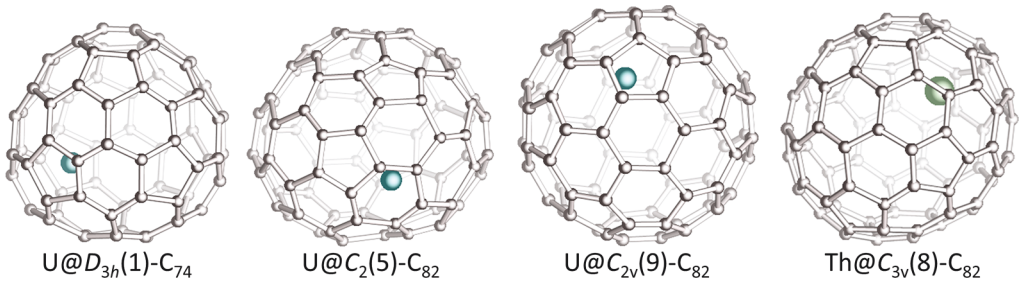

Figure 1. Single crystal X-ray structures of U@D_{3h}(1)-C_{74}, U@C_2(5)-C_{82}, U@C_{2v}(9)-C_{82}, and Th@C_{3v}(8)-C_{82}. The U atoms are highlighted in blue; the Th atom is highlighted in green.

fullerene, $Sc_3N@I_h$-C_{80}, which is still the most abundant endohedral fullerene that can be prepared in an arc reactor and third most abundant fullerene, after C_{60} and C_{70}.[3] The many studies of endohedral metallofullerenes (EMFs) during the past two decades have shown that these carbon cages are ideal molecular nanocontainers that can stabilize isolated metal atoms and reactive metal clusters and even some molecules.[4] The resulting EMFs exhibit unique electronic properties and novel bonding motifs that have potential applications in the photovoltaic and biomedical fields.[4] Recently, the successful synthesis and systematic studies of actinide-based EMFs revealed their unique electronic configurations and physicochemical properties, which are substantially different from those of the extensively investigated lanthanide-based EMFs.[5−9]

2. RECENT ADDITIONS TO THE EMF FAMILY: ACTINIDE-BASED METALLOFULLERENES

Compared to the intensively investigated lanthanide-based EMFs, actinide-based EMFs remain largely unexplored. Our recent studies of actinide-based EMFs have revealed their complex electronic structures and unexpected bonding motifs, which have never been observed for lanthanide EMFs. Moreover, the unique actinide clusters observed only inside the fullerene cages show that the host−guest structures of actinide EMFs provide multiple opportunities to study the bonding nature between actinides and ligands in an isolated and inert environment.

2.1. New Electronic Structures

One of the interesting and general features of EMFs is the high degree of metal-to-cage charge transfer, which not only affects the stability of the compounds but also influences their chemical reactivity.[10] When compared to lanthanide elements, the early actinides (Th−Pu) are highly redox active, and some of them exhibit multiple accessible oxidation states. For instance, uranium oxidation states typically range between U(III) and U(VI), while U(II) has also been reported.[11−13] In principle, uranium offers five accessible oxidation states, in contrast with the rather limited Ln(II)/Ln(III) oxidation states of the rare-earth elements. Additionally, the 5f-orbitals of the actinides are chemically accessible,[11,14] contrasting the core-like 4f-orbitals of the lanthanides. In principle, these features should result in new cage isomer preferences and in novel electronic structures for actinide EMFs. However, perhaps due to the inherent radioactivity of the actinide elements, the investigation of actinide EMFs has been mainly limited to theoretical calculations and to a few spectroscopic investigations.[15−19]

Recently, systematic experimental studies of actinide-based EMFs combined with theoretical calculations have considerably deepened our knowledge about the electronic structure of actinide-based EMFs. For the first time, the molecular structure of an actinide EMF, Th@C_{3v}(8)-C_{82}, was obtained from X-ray crystallographic analysis (Figure 1). The combined experimental and theoretical results confirmed that Th@C_{3v}(8)-C_{82} is the first example of an isolated mono-EMF with a formal four electron transfer from the metal to the cage, possessing a surprisingly large electrochemical band gap of 1.51 eV.[5] More surprisingly, the very recent discovery of $U_2C@I_h$(7)-C_{80} revealed that U can take a formal 5+ charge state in the encapsulated cluster, see details below.[7] These results illustrate the rich redox properties of the actinide EMFs compared to those of the lanthanide analogues.

Since the detection of the first endohedral metallofullerene (EMF), La@C_{82}, in 1991, it has become doctrine that the oxidation state of a given encapsulated metal (group 2, group 3, or lanthanides) is always the same, regardless of the cage size or geometry of the corresponding fullerene cages. However, single crystal X-ray structures and theoretical studies of three new U-EMFs, U@D_{3h}-C_{74}, U@C_2(5)-C_{82}, and U@C_{2v}(9)-C_{82}, revealed a unique cage isomer dependent charge transfer from the encaged U. It was shown that the oxidation state of U in two U@C_{82} isomers, U@C_2(5)-C_{82} and U@C_{2v}(9)-C_{82}, were 4+ and 3+, respectively, (Figure 1).[20] For U@D_{3h}-C_{74}, the formal oxidation state for U was also found to be 4+. These differences were attributed to variable interactions of the metal 5f orbitals with specific segments of the isomeric carbon cages.[20]

2.2. Specific Cage Isomer Preferences

For EMFs, the cage isomer preferences by the encapsulated metal ion or cluster are generally dictated by the specific metal-to-cage charge transfer as well as by the size and the geometric structures of the clusters. The unique four electron metal-to-cage charge transfer observed exclusively for the actinide mono-EMFs (M@C_{2n}) should lead to unconventional cage isomer preferences, different from those observed for the lanthanide analogues (Ln@C_{2n}). Even when compared to other EMFs that host tetravalent clusters, such as Sc_2O, Sc_2C_2, and Sc_2S, given the large geometric differences between the single metal and the metal clusters, the host−guest interactions should be substantially different. In turn, these differences should lead to completely different cage isomer preferences. The recent report of the U@C_1(17418)-C_{76}, U@C_1(28324)-C_{80}, and Th@C_1(28324)-C_{80}, which possess new non-IPR fullerene cage isomers that had never been reported before, confirms the unique cage preference by the encapsulated actinide single metals (Figure 2). DFT calculations show that a

DOI: 10.1021/acs.accounts.9b00229
Acc. Chem. Res. 2019, 52, 1824−1833

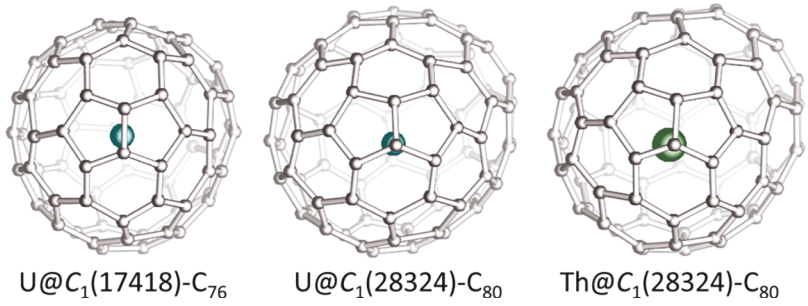

Figure 2. Single crystal X-ray structures of U@C_1(17418)-C_{76}, U@C_1(28324)-C_{80}, and Th@C_1(28324)-C_{80}. The U atoms are highlighted in blue; the Th atom is highlighted in green.

substantial part of the stabilization of these unique non-IPR actinide EMFs originates from a formal four electron transfer from the metal to the cage and from a significant degree of covalency between the actinide ions and the non-IPR fullerene cages (Figure 2), which is found to be higher for U than for Th.[6] As an early actinide, Th interacts with the fullerene via 6d and 5f orbitals in an approximately similar proportion, but U interacts mainly via the 5f orbitals, as recently observed.[21] In spite of this significant actinide−cage interaction, the actinide exhibits high mobility inside the fullerene at high temperatures (2000 K).[6] This high mobility makes both the symmetry of the carbon cage and the possibility of forming chiral fullerenes important factors to determine the observed isomer abundances at temperatures of fullerene formation (1500−3000 K).[2] In other words, low-symmetry chiral cages are thermodynamically favored at high temperatures versus nonchiral cages with high symmetry. This is the reason why the chiral and non-IPR actinide EMFs U@C_1(17418)-C_{76}, U@C_1(28324)-C_{80}, and Th@C_1(28324)-C_{80} are favored during the formation process. Notably, such covalent stabilization factors had never been previously observed, although Sm@C_{2v}(19138)-C_{76} was the first reported mono-EMF with a non-IPR cage.[22] However, it is worth noting that the probability of capturing non-IPR cages would be very small if there were a relatively high number of available IPR isomers with C_1 symmetry. In this case, IPR cages with relatively high symmetry would be preferentially formed during the arc-discharge process if their relative energies were large enough. The prototypical example of this situation is U@D_{3h}-C_{74}.[20] The D_{3h}-C_{74} cage still exhibits much higher stability relative to the other three C_{74} isomers when U is encapsulated, due to a very short uranium−fullerene bond distance. Accordingly, D_{3h}-C_{74} is the dominant isomer up to 2800 K, because neither thermal nor entropic effects can compensate for the energy differences.

2.3. Actinide Clusters with Novel Bonding Motifs

To date, even though the nature of actinide−actinide and non-metal−actinide bonds has attracted considerable attention, difficulties with the syntheses and characterization have hindered their exploration using conventional synthetic actinide chemistry. As already mentioned, one of the most interesting features of EMFs is the significant charge transfer that occurs from the encapsulated ions or clusters to the cages. Some metal clusters with unique electronic configurations, which otherwise are not stable, can be stabilized upon encapsulation due to the charge transfer process. The recent success in isolating new actinide metallic cluster endohedral fullerenes proved that fullerene cages can act as unique and effective nanocontainers to encapsulate and stabilize unexpected bonding motifs for new actinide clusters. Combined experimental and computational studies focusing particularly on the electronic structures of these bonding motifs have provided a deeper understanding of actinide−actinide and non-metal−actinide bonds.

Compared to the extensive studies of lanthanide−lanthanide bonding inside fullerene cages, such as La−La, Sc−Sc, Y−Y, Tb−Tb, Lu−Lu, and Dy−Dy single bonds, the possibility of forming U−U bonds inside fullerene cages had only been considered by theoreticians until very recently.[23−30] Wu and Lu suggested that a 6-fold U−U bond could exist inside a C_{60} cage, whereas Gagliardi et al. argued that such bonding results from the constrictive size of the C_{60} cage since the two U atoms prefer to be more separated in larger fullerene cages.[31,32] Interestingly, even though Straka et al. predicted the existence of U−U bonds in a series of $U_2@C_{2n}$ ($2n$ = 70, 80, 84), they still described such a U−U endohedral bond as "unwilling", meaning that the bonding results from the cage compression effect and the need to decrease the charge−charge repulsion between the encapsulated atoms.[33] Despite all the theoretical arguments, no experimental data for a dimetallic actinide EMF had been obtained until recently, when the synthesis, isolation, and full characterization of $U_2@I_h(7)$-C_{80} was reported (Figure 3a).[8] Crystallographic, spectroscopic, and computational studies of this EMF confirmed that the two U atoms adopt a formal 3+ oxidation state, thus formally transferring 6 electrons to the $I_h(7)$-C_{80} cage. In particular, the crystallographic structure showed that the U···U distances between the two U atoms are in the range of 3.46−3.79 Å, a distance range that is shorter than that predicted theoretically (3.9 Å).[33] For the

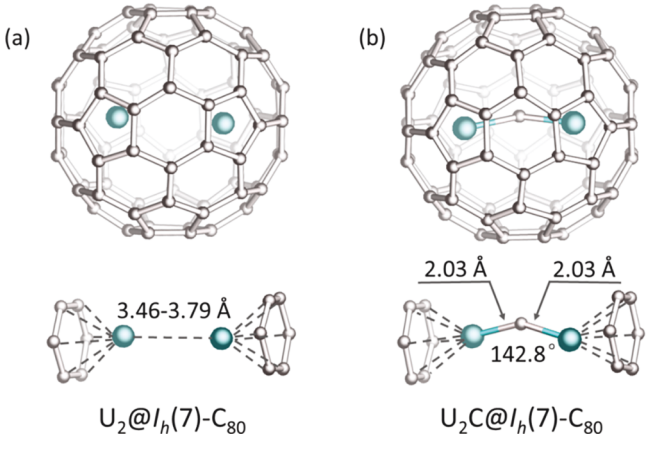

Figure 3. Single crystal X-ray structures of (a) $U_2@I_h(7)$-C_{80} and (b) $U_2C@I_h(7)$-C_{80}. The U atoms are highlighted in blue.

DOI: 10.1021/acs.accounts.9b00229
Acc. Chem. Res. 2019, 52, 1824−1833

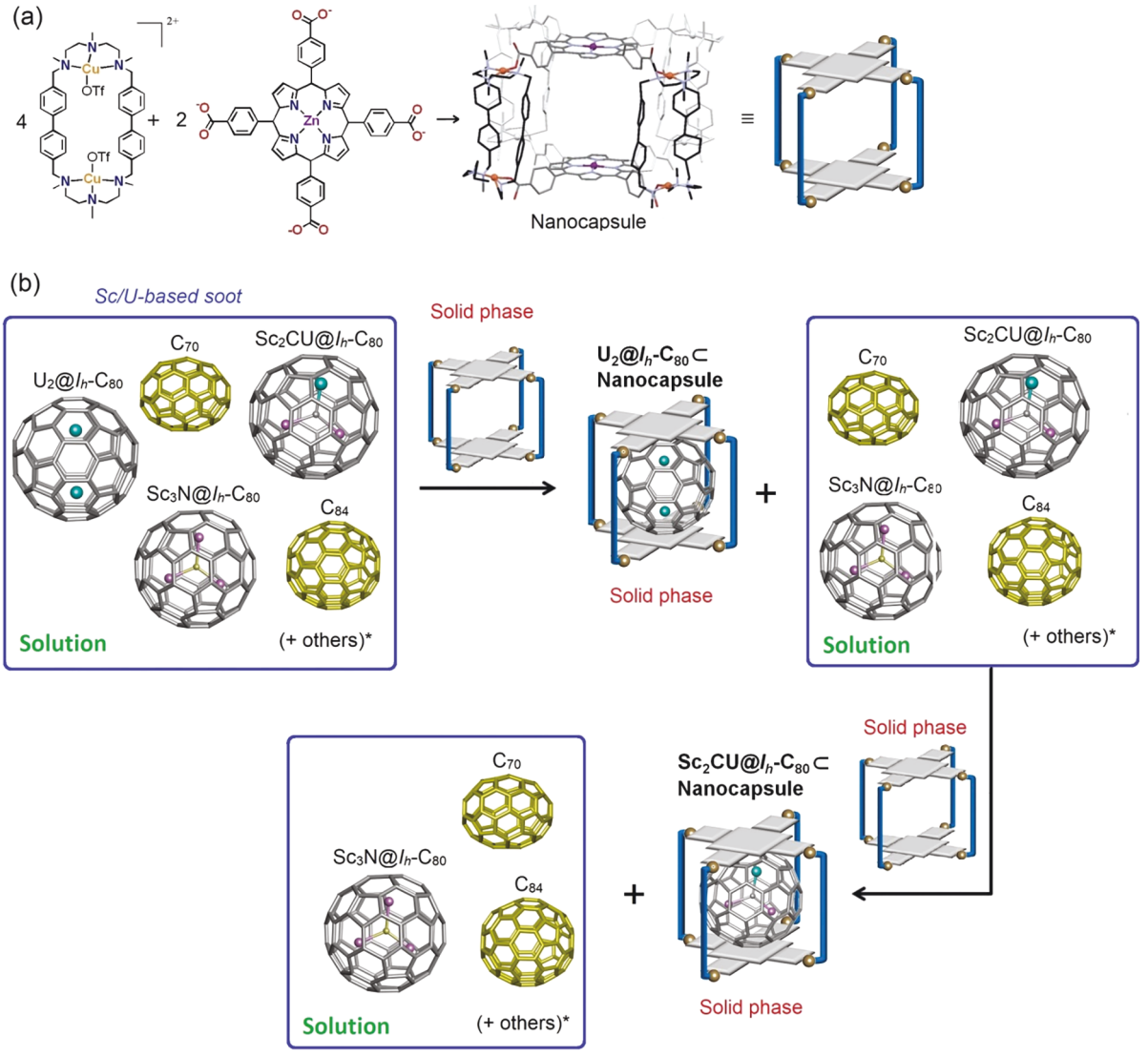

Figure 4. (a) Synthesis of self-assembled Cu-based supramolecular nanocapsules. Cu atoms are denoted by orange balls, and Zn atoms are denoted by purple balls. Reprinted with permission from ref 38. Copyright 2018 WILEY-VCH. (b) Selective sequential encapsulation of $U_2@I_h(7)$-C_{80} first and then $Sc_2CU@C_{80}$ from raw soot using the Cu-based nanocapsule (*other endohedral metallofullerenes are present in the soot in small amounts).[38]

first time these results provided experimental evidence for the existence of a weak U−U bonding interaction. Further experimental work with different sized fullerene cages will further explore this unique bonding motif, which has only been observed inside the I_h-C_{80} fullerene cage so far.

Interestingly, some fullerene cages were able to stabilize some rather unexpected and unconventional actinide metal clusters. $UCU@I_h(7)$-C_{80} is the first and only actinide metallic cluster EMF reported to date (Figure 3b).[7] In this unusual EMF, an unprecedented cage-stabilized bent UCU cluster with unexpectedly short uranium−carbon distances (2.03 Å) was found to be stabilized inside an $I_h(7)$-C_{80} fullerene cage. This result demonstrates the importance of actinide metallic cluster EMF work for expanding fullerene chemistry and understanding fundamental actinide bonding properties. In the EMF field, $M_2C@I_h$-C_{80} is an unexpected endohedral structure, which had never been observed before for any metal. Moreover, in $UCU@I_h(7)$-C_{80}, U adopts a formal 5+ oxidation state, which is also unprecedented for metal clusters encapsulated inside fullerene cages. The variety of oxidation states observed for U shows that actinide metallic cluster EMFs are substantially different from lanthanide metallic cluster EMFs. Extended studies of actinide metallic cluster EMFs will likely lead to important new clusters and structures that will provide fundamental insights and knowledge about chemical bonding. From the viewpoint of actinide chemistry, even though metal−carbon double bonds are common in transition metal chemistry and catalysis, unsupported U═C bonds were not well characterized for molecular uranium complexes, specifically those that lack ancillary heteroatom or chelating supporting groups. The U═C bond in the encapsulated U═C═U cluster represents the first structurally characterized example of unsupported axial uranium U═C double bonds (Figure 3b). This finding in fact confirmed the distinction between "axial" covalent and "equatorial" dative bonding mechanisms for uranium, which was proposed by theoreticians some time ago.[34] It is interesting to note that the U−U distances for $U_2@I_h(7)$-C_{80} (3.46−3.79 Å) and $U_2C@I_h(7)$-C_{80} (3.849 Å) are similar to each other, but the bonding interactions are totally different.

DOI: 10.1021/acs.accounts.9b00229
Acc. Chem. Res. 2019, 52, 1824−1833

2.4. Porphyrin-based Nanocapsules Selectively Bind Different U-EMFs

Until now, the HPLC separation method is the most-utilized technique for the purification of EMFs, but it is also a very time and solvent consuming procedure. Therefore, researchers have attempted to develop efficient HPLC-free purification methods for a long time.[35,36] In 2017, Ribas, Echegoyen, and co-workers reported a self-assembled copper-based supramolecular nanocapsule, fabricated by two tetracarboxylate Zn(II)-porphyrin segments and four Cu(II)-based macrocyclic clips (see structures in Figure 4).[37] The four accessible portals of this nanocapsule were designed to allow easy exchange of fullerenes from the inside of the cavity to the outside solution (Figure 4a). It was found that for a mixture containing empty fullerenes (C_{60} and C_{70}) and Sc_3N-based endohedral metallofullerenes ($Sc_3N@I_h$-C_{80} and $Sc_3N@D_{5h}$-C_{80}), the smaller fullerenes were trapped inside the crystals of the nanocapsule, while the larger $Sc_3N@C_{80}$ (I_h and D_{5h} isomer) remained in solution. Based on these size-dependent differential affinities, it was possible to separate the smaller cages from $Sc_3N@C_{80}$, which was obtained in 99.5% purity. Very recently, this nanocapsule was successfully applied for the selective separation of a series of U-based actinide EMFs from a U/Sc-based soot. The nanocapsule crystals were soaked in a toluene solution of soot extract containing C_{70}, $Sc_3N@I_h(7)$-C_{80}, $U_2@I_h(7)$-C_{80}, and $Sc_2CU@$-C_{80}, and $U_2@I_h(7)$-C_{80} was selectively absorbed in the soaked crystal (Figure 4b). This degree of selective binding is remarkable and has provided an easy and convenient method for the isolation of pure $U_2@I_h(7)$-C_{80} in a single step. Subsequently, the residual mixture of empty and endohedral fullerenes was exposed to additional nanocapsule crystals, and the unprecedented compound $Sc_2CU@C_{80}$, which represents the first example of a mixed metal actinide-based EMF, was selectively complexed.[38] This stepwise heterogeneous process for actinide endohedral purification yields two pure compounds, $U_2@I_h(7)$-C_{80} and $Sc_2CU@C_{80}$, in a very convenient extraction method, from an initial rather complex soot sample. These results demonstrated the remarkable separation ability of these nanocapsules, which can selectively bind different EMFs containing the same C_{80} cage with different encapsulated species. DFT calculations suggest that the highly directional electron-density distribution of the U based fullerenes, induced by the host−guest interaction, is likely to be the origin of this subtle discrimination ability. It is important to mention that all encapsulated fullerenes were easily released by a solvent-washing procedure, which makes this straightforward methodology promising for the practical and nonchromatographic purification of EMFs.

3. MECHANISTIC INSIGHTS OF THE BOTTOM-UP GROWTH PROCESSES DURING EMF FORMATION

Although the formation processes of EMFs have not been clearly elucidated, two different mechanistic proposals for EMF formation and growth, namely, top-down and bottom-up processes, have been proposed. The top-down mechanistic proposal postulates that smaller fullerene cages can be formed via a cascade of C_2 extrusions from larger fullerene cages or even from graphene. A mono-EMF, $Eu@C_{88}$, and two carbide cluster endohedral fullerenes, $Gd_2C_2@C_1(51383)$-C_{84} and $La_2C_2@C_2(816)$-C_{104}, have crystallographic structures that support the top-down formation mechanism.[39−41] These cages are proposed to be intermediates along the formation pathways for fullerenes with either IPR or non-IPR cages.

In addition to the top-down process, Kroto and colleagues have proposed that metallofullerenes may form through an alternate, bottom-up formation mechanism.[42−44] They showed that metallofullerenes can be formed via consecutive C_2 additions to small carbon nanoclusters and cages under a rich carbon vapor atmosphere. Consistently, large $U@C_{2n}$ EMFs can be formed starting with the smallest stable fullerene, $U@C_{28}$, as a precursor.[45] Similar bottom-up mechanisms were proposed based on mass spectral and DFT calculation studies of the $Ti@C_{2n}$ ($2n$ = 26−50) family as well.[46] However, it appears that most of the bottom-up processes are supported only by mass spectral evidence during laser ablation synthetic processes and corresponding DFT calculations. No substantial physical evidence for the bottom-up growth model was reported until the very recent work by Echegoyen, Poblet, Balch, and colleagues, in which an endohedral carbide fullerene with an unprecedented heptagon ring, $Sc_2C_2@C_s$(hept)-C_{88}, was structurally characterized. It was proposed that this nonclassical carbide cluster endohedral is a kinetically trapped intermediate in a bottom-up growth process from $Sc_2C_2@C_{2v}(9)$-C_{86} via a direct C_2 insertion (Figure 5a).[47,48] This agrees well with theoretical results, which show that insertion

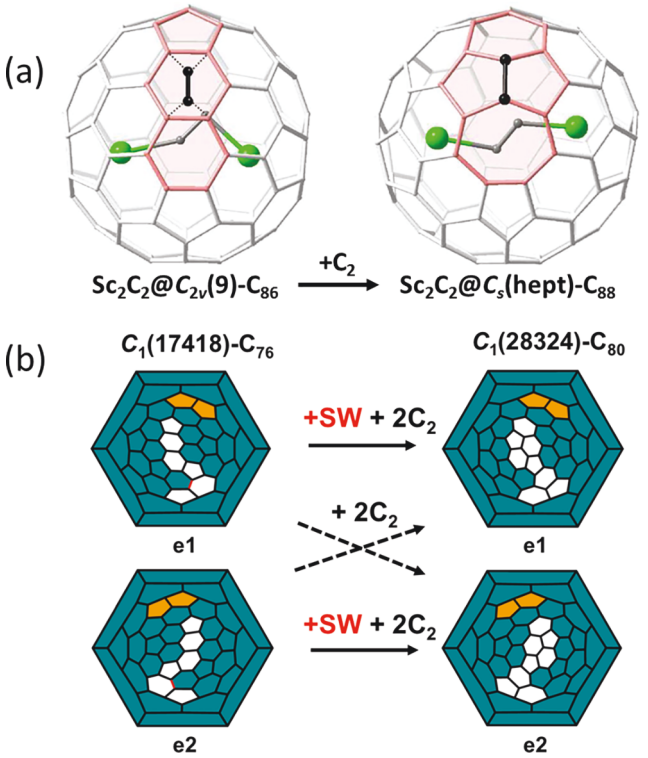

Figure 5. (a) Structural relationship between $Sc_2C_2@C_{2v}(9)$-C_{86} and $Sc_2C_2@C_s$(hept)-C_{88} by a C_2 insertion. The motif that is involved in the transformation is highlighted in pink. The inserted C_2 unit is highlighted in black. Reprinted with permission from ref 48. Copyright 2016 American Chemical Society. (b) Schlegel diagrams showing topological links between chiral $C_1(17418)$-C_{76} and $C_1(28324)$-C_{80}. The dark blue regions correspond to the common parts shared by the two cages. The pentalene is highlighted in orange. The bond that rearranges through a SW transformation is highlighted in red. Reprinted with permission from ref 6. Copyright 2018 American Chemical Society.

DOI: 10.1021/acs.accounts.9b00229
Acc. Chem. Res. 2019, 52, 1824−1833

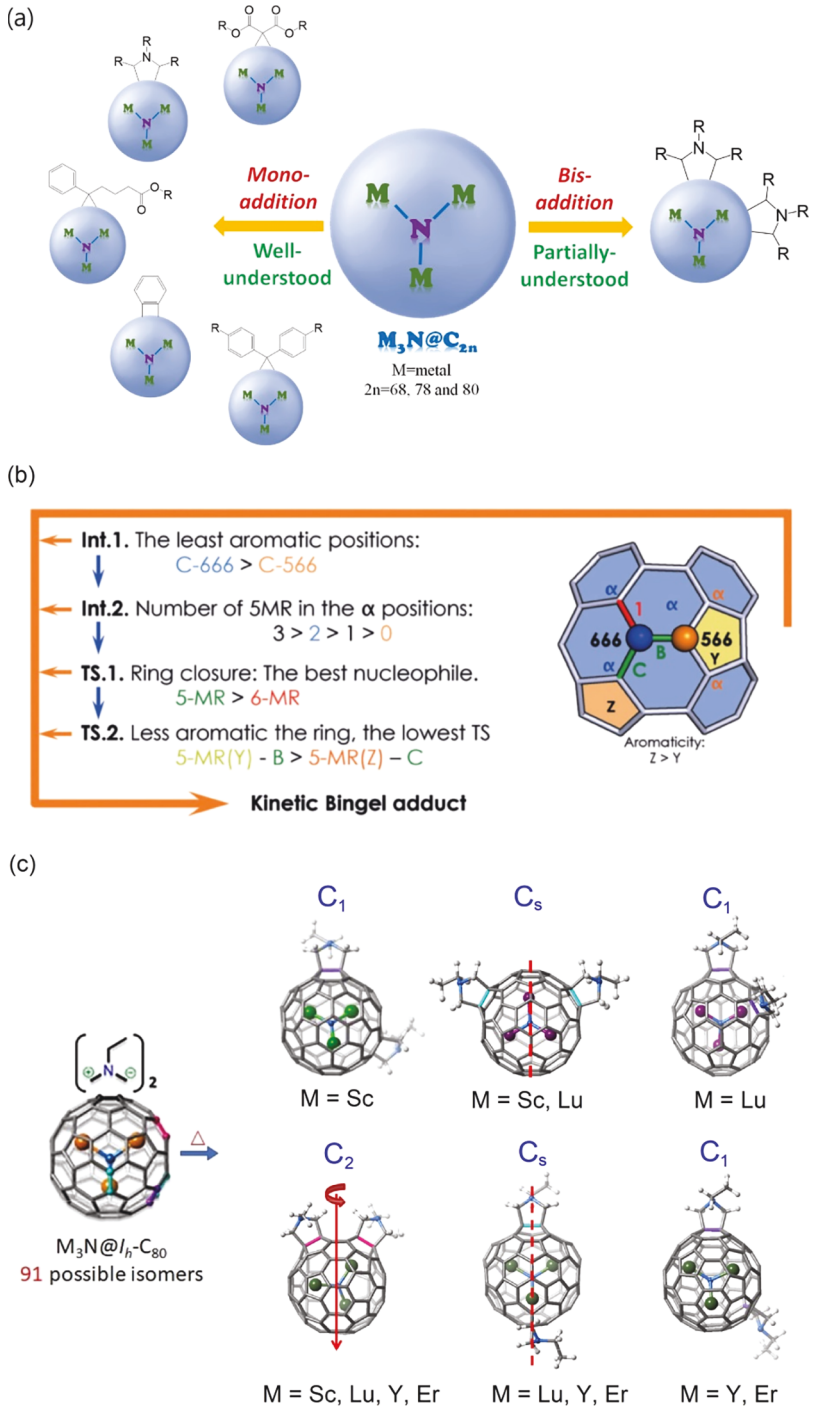

Figure 6. (a) Major types of monoaddition and bis-addition of EMFs. (b) Predictive aromaticity criteria (PAC) rule for Bingel–Hirsch addition of IPR-EMFs. Reprinted with permission from ref 50. Copyright 2016 WILEY-VCH. (c) Products of bis-1,3-dipolar cycloadditions $M_3N@I_h$-C_{80} (M = Sc, Lu, Y, and Er). Reprinted with permission from ref 52 (Copyright 2015 American Chemical Society) and ref 53 (Copyright 2017 Elsevier).

of C_2 requires less energy than the corresponding Stone–Wales rearrangements.[49] While $Sc_2C_2@C_s$(hept)-C_{88} is not the thermodynamically most stable structure calculated theoretically, four or five consecutive Stone–Wales rearrangements are necessary to transform this structure into a pentalene containing isomer or an IPR cage, respectively. The latter are thermodynamically more stable, but due to the high activation energies required to effect each Stone–Wales rearrangement, they are totally not accessible kinetically.

Our very recent study of non-IPR uranium EMFs allowed us to explore a new transformation pathway for a bottom-up growth process.[6] The topological connections between two non-IPR chiral carbon cages, C_1(17894)-C_{76} and C_1(28324)-C_{80}, are enantiomerically dependent. Specifically, enantiomer *e1* (*e2*) of C_1(17418)-C_{76} and enantiomer *e2* (*e1*) of C_1(28324)-C_{80} are topologically connected by only two C_2 insertions with no necessary Stone–Wales rearrangements (Figure 5b). These paths are less energetically demanding than those that preserve the same chirality. This work shed new

DOI: 10.1021/acs.accounts.9b00229
Acc. Chem. Res. 2019, 52, 1824–1833

light on the structural rearrangements occurring during a bottom-up growth process and leads to new mechanistic insights concerning the formation of endohedral fullerenes during the arc discharge process.

4. THE CONTROLLING INFLUENCE OF CLUSTERS ON THE REACTIVITY OF EMFs

The exohedral functionalization of the fullerene cages can be designed to fine tune the solubility and physicochemical properties of EMFs for different applications and specific purposes. The additions of single addends to EMFs have been comprehensively investigated with regard to exohedral regioselectivity and its correlation to the configurations of the inner species (Figure 6a). Solà and co-workers proposed a predictive aromaticity criterion (PAC) rule for predicting the most favorable position for Bingel−Hirsch additions of diethylbromomalonate to EMF systems obeying the isolated pentagon rule (IPR) (Figure 6b), supported by experimental data.[50] Compared to the rather well understood monoadditions to EMFs, the bis-additions remain largely unexplored. However, it is worth noting that the encapsulated clusters play a major controlling influence on the regioselectivity of the bis-addition products. For example, Yamakoshi and co-workers reported that the main bisadducts of $Y_3N@I_h$-C_{80} and $Gd_3N@I_h$-C_{80} upon 1,3-dipolar cycloaddition reactions with N-ethylglycine and formaldehyde were the kinetic [6,6]−[6,6]-bisadducts.[51] Theoretical calculations showed that the Gd_3N cluster stabilizes the kinetic [6,6]-monoadduct, and the second addition leads to the stable [6,6]−[6,6]-bisadduct. Recently, Echegoyen and co-workers analyzed and described the 91 statistical possible regioisomers for bisadditions to $M_3N@I_h$-C_{80} (M = Sc, Lu, Y, and Er).[52] Strikingly, the number of endohedral trimetallic nitride bis-pyrrolidine regioisomers is drastically reduced from the possible 91 to only 3 or 4, and thus only six types of bis-pyrrolidine products were observed (Figure 6c), evidently showing the strong directing effect of the encapsulated cluster.[52,53] In detail, the three bis-pyrrolidine bisadducts of $Sc_3N@I_h$-C_{80} compounds were determined to be [5,6]−[5,6] additions with C_1, C_s, and C_2 symmetries. Four bis-pyrrolidine regioisomers of $Lu_3N@I_h$-C_{80} were identified, a [5,6]−[5,6] addition with C_2 and C_s symmetries, a [5,6]−[5,6]-C_1-unsymmetric isomer, and the first mixed (hybrid) [5,6]−[6,6]-C_s-symmetric bisadduct regioisomer. Three bis-pyrrolidine regioisomers of $Y_3N@I_h$-C_{80} were identified as [5,6]−[5,6]-C_2-symmetric, [5,6]−[6,6]-C_s-symmetric, and [6,6]−[6,6]-C_1-unsymmetric. Finally, three bis-pyrrolidine regioisomers of $Er_3N@I_h$-C_{80} were identified as a [5,6]−[5,6]-C_2-symmetric, a [5,6]−[6,6]-C_s-symmetric, and a [6,6]−[6,6]-C_1-unsymmetric regioisomer based on the UV−vis absorption fingerprint pattern. Calculations showed that after the first addition, the cluster reduces its mobility and is largely localized, resulting in increased pyramidalization of only select carbons on the cage. These carbons are the most reactive sites and correspond to the few bisadduct regioisomers that are experimentally observed.

5. CONCLUSIONS AND FUTURE PERSPECTIVE

The interior spaces inside fullerene carbon cages have provided a wealth of structurally and electronically unique cavities that lead to encapsulation of a wide variety of species, ranging from single atoms and ions to more complex clusters and intact molecules. The host−guest interactions between the cages and their trapped species lead to interesting structures and properties and to the observation of endohedral chemical species that are not synthetically available outside of these rigid carbon cages. In this Account, we summarized the latest progress on the study of different types of new EMFs as well as their chemical reactivity. In particular, we described the syntheses and characterizations of a new family of EMFs that contain actinide metals inside. The actinide EMFs show substantial differences of their metal oxidation states, degrees of metal-to-cage charge transfer, and cage isomer preferences when compared to those of the more classic lanthanide-based EMFs. The formal oxidation states thus far characterized for U EMFs range from 3+ to 5+, and isomeric cages exhibit different values, an observation never before reported. Some long-sought bonding motifs in actinide chemistry were observed for the first time in encapsulated structures of the actinide EMFs, with the fullerenes acting as exotic nanocontainers. A weak ∼3.7 Å U−U bond was characterized inside a C_{80} cage for $U_2@I_h(7)$-C_{80} and a never before observed or even theorized cluster, U═C═U, was also observed inside the same carbon isomer cage. The latter exhibits two 2.03 Å unsupported U═C double bonds, an exotic but fundamentally important cluster. Changing the heteroatom in U═X═U from X = C to other elements will help increase fundamental knowledge about U and the bonding motifs of the encapsulated actinide metal clusters. At the same time, changing the size and isomer of the fullerene cage around the U═X═U will help to understand the intrinsic properties of these unusual compounds. Our progress suggests that, as a largely unexplored research area, actinide EMF studies have significance for fundamental actinide chemistry as well as for fullerene research. Future work should continue to focus on their novel structures, their bonding motifs, and more importantly, their novel material properties, for example, molecular magnetism, which could be a result of their unique electronic structures. The characterization of actinide EMFs shows that different metals encapsulated can lead to fundamentally different physical and chemical properties resulting from their unique electronic structures, which is encouraging for the future exploration of novel EMFs with other types of metals encapsulated.

In addition, novel carbide EMF structures, for example, $Sc_2C_2@C_s$(hept)-C_{88}, were proposed as key intermediate products in a bottom-up growth process of EMF formation. These results suggest that more intermediate structures likely exist, which remain unknown to date, that could be stabilized by various metal clusters. The continued exploration of these novel EMF structures may fill the missing pieces in the proposed growth maps, which will eventually provide solid evidence for a reliable growth mechanism of EMFs. Improved understanding of the mechanistic pathways for endohedral fullerene formation will lead to optimized synthetic conditions that will afford increased yields and new structures with unusual properties. Our studies also suggest that the encapsulated clusters exert a major controlling influence on the regioselectivity of multiple exohedral addition products. Fundamental understanding of the interplay between endohedral clusters and exohedral functionalization has relevance in the field of graphene, where interactions between chemical groups across a single carbon layer are very important. Our endohedral compounds provide a unique platform to probe these interactions across a single fullerene carbon layer. Future studies may be devoted to developing methodologies to control and fine-tune exohedral additions to prepare

DOI: 10.1021/acs.accounts.9b00229
Acc. Chem. Res. 2019, 52, 1824−1833

customized EMFs for applications in fields such as quantum spintronics and biomedicine.

AUTHOR INFORMATION

Corresponding Authors

*E-mail: echegoyen@utep.edu.
*E-mail: chenning@suda.edu.cn.

ORCID

Wenting Cai: 0000-0003-3653-1711
Chia-Hsiang Chen: 0000-0003-3489-4316
Ning Chen: 0000-0002-9405-6229
Luis Echegoyen: 0000-0003-1107-9423

Author Contributions

‡W.C. and C.-H.C. contributed equally to this work.

Notes

The authors declare no competing financial interest.

Biographies

Wenting Cai obtained her Ph.D. under the supervision of Professor Xing Lu from Huazhong University of Science and Technology in 2015. From 2012 to 2013, she studied in the group of Professor Takeshi Akasaka at University of Tsukuba, as a visiting Ph.D. student. She is now working as a postdoctoral researcher with Prof. Luis Echegoyen at University of Texas at El Paso. Her research interests include the generation and characterization of novel metallofullerenes.

Chia-Hsiang Chen received his Ph.D. degree from the National Sun Yat-Sen University in 2012, under the supervision of Professor Wen-Yann Yeh. After working as a postdoctoral fellow with Prof. Luis Echegoyen from 2013 to 2015 at University of Texas at El Paso and with Dr. Alexey A. Popov at Leibniz Institute for Solid State and Materials Research from 2015 to 2018, he joined the Kaohsiung Medical University as an assistant professor in 2018. His current research interests include the coordination chemistry of fullerenes, endohedral metallofullerenes, and nanographene.

Ning Chen is a professor in the College of Chemistry, Chemical Engineering and Materials Science, Soochow University. He obained his Ph.D. degree from the Institute of chemistry, Chinese Academy of Science, in 2007 under the supervision of Prof. Chunru Wang. He went on to do postdoctoral research with Prof. Lothar Dunsch at Leibniz Institute for Solid State and Materials Research from 2007 to 2009. He continued to work with Prof. Luis Echegoyen as a postotoral researcher first at Clemson Univeristy then at Uniersity of Texas at El Paso from 2009 to 2012. From 2012, he started his independent career at Soochow University. His research interests are focused on novel endohedral fullerenes, fullerene derivatives, and their applications on photovoltaic devices.

Luis Echegoyen was born in La Habana, Cuba, in 1951. He obtained both his B.Sc. and Ph.D. from the University of Puerto Rico in Rio Piedras (1971 and 1974, respectively). After an industrial placement at Union Carbide and several professorships at the Universities of Puerto Rico, Maryland, and Miami, in 2002 he was appointed as Chair of the Department of Chemistry at Clemson University, in South Carolina. Later, he served as Division Director for Chemistry at the National Science Foundation for 4 years (2006−2010), and he became the Robert A. Welch Professor of Chemistry at the University of Texas at El Paso in 2010. More recently, he was elected the 2019 American Chemical Society president-elect and will serve as president in 2020. His research interests include fullerene chemistry, electrochemistry, and supramolecular chemistry, with special emphasis in photovoltaics and endohedral fullerenes.

ACKNOWLEDGMENTS

We thank Dr. Antonio Rodríguez Fortea (Universitat Rovira I Virgili) for insightful discussion and help on revisions. L.E. thanks the Robert A. Welch Foundation for an endowed chair and Grant No. AH-0033 and the U.S. NSF (Grant No. CHE-1801317) for generous financial support. N.C. thanks the National Science Foundation China (NSFC 51302178), the NSF of Jiangsu Province (BK20171211), Priority Academic Program Development of Jiangsu Higher Education Institutions (PAPD), and the project of scientific and technologic infrastructure of Suzhou (SZS201708).

REFERENCES

(1) Heath, J. R.; O'Brien, S. C.; Zhang, Q.; Liu, Y.; Curl, R. F.; Tittel, F. K.; Smalley, R. E. Lanthanum complexes of spheroidal carbon shells. *J. Am. Chem. Soc.* **1985**, *107*, 7779−7780.

(2) Krätschmer, W.; Lamb, L. D.; Fostiropoulos, K.; Huffman, D. R. Solid C_{60}: a new form of carbon. *Nature* **1990**, *347*, 354−358.

(3) Stevenson, S.; Rice, G.; Glass, T.; Harich, K.; Cromer, F.; Jordan, M. R.; Craft, J.; Hadju, E.; Bible, R.; Olmstead, M. M.; Maitra, K.; Fisher, A. J.; Balch, A. L.; Dorn, H. C. Small-bandgap endohedral metallofullerenes in high yield and purity. *Nature* **1999**, *401*, 55.

(4) Popov, A. A.; Yang, S.; Dunsch, L. Endohedral Fullerenes. *Chem. Rev.* **2013**, *113*, 5989−6113.

(5) Wang, Y.; Morales-Martínez, R.; Zhang, X.; Yang, W.; Wang, Y.; Rodríguez-Fortea, A.; Poblet, J. M.; Feng, L.; Wang, S.; Chen, N. Unique Four-Electron Metal-to-Cage Charge Transfer of Th to a C_{82} Fullerene Cage: Complete Structural Characterization of Th@$C_{3v}(8)$-C_{82}. *J. Am. Chem. Soc.* **2017**, *139*, 5110−5116.

(6) Cai, W.; Abella, L.; Zhuang, J.; Zhang, X.; Feng, L.; Wang, Y.; Morales-Martínez, R.; Esper, R.; Boero, M.; Metta-Magaña, A.; Rodríguez-Fortea, A.; Poblet, J. M.; Echegoyen, L.; Chen, N. Synthesis and Characterization of Non-Isolated-Pentagon-Rule Actinide Endohedral Metallofullerenes U@$C_1(17418)$-C_{76}, U@$C_1(28324)$-C_{80}, and Th@$C_1(28324)$-C_{80}: Low-Symmetry Cage Selection Directed by a Tetravalent Ion. *J. Am. Chem. Soc.* **2018**, *140*, 18039−18050.

(7) Zhang, X.; Li, W.; Feng, L.; Chen, X.; Hansen, A.; Grimme, S.; Fortier, S.; Sergentu, D.-C.; Duignan, T. J.; Autschbach, J.; Wang, S.; Wang, Y.; Velkos, G.; Popov, A. A.; Aghdassi, N.; Duhm, S.; Li, X.; Li, J.; Echegoyen, L.; Schwarz, W. H. E.; Chen, N. A diuranium carbide cluster stabilized inside a C_{80} fullerene cage. *Nat. Commun.* **2018**, *9*, 2753.

(8) Zhang, X.; Wang, Y.; Morales-Martínez, R.; Zhong, J.; de Graaf, C.; Rodríguez-Fortea, A.; Poblet, J. M.; Echegoyen, L.; Feng, L.; Chen, N. U_2@$I_h(7)$-C_{80}: Crystallographic Characterization of a Long-Sought Dimetallic Actinide Endohedral Fullerene. *J. Am. Chem. Soc.* **2018**, *140*, 3907−3915.

(9) Zhang, J.; Stevenson, S.; Dorn, H. C. Trimetallic Nitride Template Endohedral Metallofullerenes: Discovery, Structural Characterization, Reactivity, and Applications. *Acc. Chem. Res.* **2013**, *46*, 1548−1557.

(10) Campanera, J. M.; Bo, C.; Poblet, J. M. General Rule for the Stabilization of Fullerene Cages Encapsulating Trimetallic Nitride Templates. *Angew. Chem., Int. Ed.* **2005**, *44*, 7230−7233.

(11) Liddle, S. T. The Renaissance of Non-Aqueous Uranium Chemistry. *Angew. Chem., Int. Ed.* **2015**, *54*, 8604−8641.

(12) MacDonald, M. R.; Fieser, M. E.; Bates, J. E.; Ziller, J. W.; Furche, F.; Evans, W. J. Identification of the + 2 Oxidation State for Uranium in a Crystalline Molecular Complex, [K(2.2.2-Cryptand)]-[$(C_5H_4SiMe_3)_3$U]. *J. Am. Chem. Soc.* **2013**, *135*, 13310−13313.

(13) La Pierre, H. S.; Scheurer, A.; Heinemann, F. W.; Hieringer, W.; Meyer, K. Synthesis and Characterization of a Uranium(II) Monoarene Complex Supported by δ Backbonding. *Angew. Chem., Int. Ed.* **2014**, *53*, 7158−7162.

(14) Hayton, T. W. Recent developments in actinide-ligand multiple bonding. *Chem. Commun.* **2013**, *49*, 2956−2973.

DOI: 10.1021/acs.accounts.9b00229
Acc. Chem. Res. 2019, 52, 1824−1833

(15) Guo, T.; Diener, M.; Chai, Y.; Alford, M.; Haufler, R.; McClure, S.; Ohno, T.; Weaver, J.; Scuseria, G.; Smalley, R. Uranium Stabilization of C_{28}: A Tetravalent Fullerene. *Science* **1992**, *257*, 1661−1664.
(16) Akiyama, K.; Zhao, Y. L.; Sueki, K.; Tsukada, K.; Haba, H.; Nagame, Y.; Kodama, T.; Suzuki, S.; Ohtsuki, T.; Sakaguchi, M.; Kikuchi, K.; Katada, M.; Nakahara, H. Isolation and characterization of light actinide metallofullerenes. *J. Am. Chem. Soc.* **2001**, *123*, 181−182.
(17) Akiyama, K.; Sueki, K.; Tsukada, K.; Yaita, T.; Miyake, Y.; Haba, H.; Asai, M.; Kodama, T.; Kikuchi, K.; Ohtsuki, T.; Nagame, Y.; Katada, M.; Nakahara, H. Study of Metallofullerenes Encapsulating Actinides. *J. Nucl. Radiochem. Sci.* **2002**, *3*, 151−154.
(18) Akiyama, K.; Sueki, K.; Haba, H.; Tsukada, K.; Asai, M.; Yaita, T.; Nagame, Y.; Kikuchi, K.; Katada, M.; Nakahara, H. Production and characterization of actinide metallofullerenes. *J. Radioanal. Nucl. Chem.* **2003**, *255*, 155−158.
(19) Liu, X.; Li, L.; Liu, B.; Wang, D.; Zhao, Y.; Gao, X. Theoretical Study on the Ground State Structure of Uranofullerene U@C_{82}. *J. Phys. Chem. A* **2012**, *116*, 11651−11655.
(20) Cai, W.; Morales-Martínez, R.; Zhang, X.; Najera, D.; Romero, E. L.; Metta-Magaña, A.; Rodríguez-Fortea, A.; Fortier, S.; Chen, N.; Poblet, J. M.; Echegoyen, L. Single crystal structures and theoretical calculations of uranium endohedral metallofullerenes (U@C_{2n}, 2n = 74, 82) show cage isomer dependent oxidation states for U. *Chem. Sci.* **2017**, *8*, 5282−5290.
(21) Muñoz-Castro, A.; Bruce King, R. Evaluation of bonding, electron affinity, and optical properties of M@C_{28} (M = Zr, Hf, Th, and U): Role of d- and f-orbitals in endohedral fullerenes from relativistic DFT calculations. *J. Comput. Chem.* **2017**, *38*, 44−50.
(22) Hao, Y. J.; Feng, L.; Xu, W.; Gu, Z. G.; Hu, Z. Q.; Shi, Z. J.; Slanina, Z.; Uhlik, F. Sm@C_{2v} (19138)-C_{76}: A Non-IPR Cage Stabilized by a Divalent Metal Ion. *Inorg. Chem.* **2015**, *54*, 4243−4248.
(23) Popov, A.; Avdoshenko, S. M.; Pendas, A. M.; Dunsch, L. Bonding between strongly repulsive metal atoms: an oxymoron made real in a confined space of endohedral metallofullerenes. *Chem. Commun.* **2012**, *48*, 8031−8050.
(24) Zuo, T. M.; Xu, L. S.; Beavers, C. M.; Olmstead, M. M.; Fu, W. J.; Crawford, D.; Balch, A. L.; Dorn, H. C. M_2@C_{79}N (M = Y, Tb): Isolation and characterization of stable endohedral metallofullerenes exhibiting M-M bonding interactions inside aza[80]fullerene cages. *J. Am. Chem. Soc.* **2008**, *130*, 12992−12997.
(25) Umemoto, H.; Ohashi, K.; Inoue, T.; Fukui, N.; Sugai, T.; Shinohara, H. Synthesis and UHV-STM observation of the T-d-symmetric Lu metallofullerene: Lu_2@C_{76}(T_d). *Chem. Commun.* **2010**, *46*, 5653−5655.
(26) Liu, F.; Krylov, D. S.; Spree, L.; Avdoshenko, S. M.; Samoylova, N. A.; Rosenkranz, M.; Kostanyan, A.; Greber, T.; Wolter, A. U. B.; Büchner, B.; Popov, A. A. Single molecule magnet with an unpaired electron trapped between two lanthanide ions inside a fullerene. *Nat. Commun.* **2017**, *8*, 16098.
(27) Yamada, M.; Kurihara, H.; Suzuki, M.; Saito, M.; Slanina, Z.; Uhlik, F.; Aizawa, T.; Kato, T.; Olmstead, M. M.; Balch, A. L.; Maeda, Y.; Nagase, S.; Lu, X.; Akasaka, T. Hiding and Recovering Electrons in a Dimetallic Endohedral Fullerene: Air-Stable Products from Radical Additions. *J. Am. Chem. Soc.* **2015**, *137*, 232−238.
(28) Bao, L.; Chen, M.; Pan, C.; Yamaguchi, T.; Kato, T.; Olmstead, M. M.; Balch, A. L.; Akasaka, T.; Lu, X. Crystallographic Evidence for Direct Metal−Metal Bonding in a Stable Open-Shell La_2@I_h-C_{80} Derivative. *Angew. Chem., Int. Ed.* **2016**, *55*, 4242−4246.
(29) Shen, W.; Bao, L.; Wu, Y.; Pan, C.; Zhao, S.; Fang, H.; Xie, Y.; Jin, P.; Peng, P.; Li, F.-F.; Lu, X. Lu_2@C_{2n} (2n = 82, 84, 86): Crystallographic Evidence of Direct Lu−Lu Bonding between Two Divalent Lutetium Ions Inside Fullerene Cages. *J. Am. Chem. Soc.* **2017**, *139*, 9979−9984.
(30) Pan, C.; Shen, W.; Yang, L.; Bao, L.; Wei, Z.; Jin, P.; Fang, H.; Xie, Y.; Akasaka, T.; Lu, X. Crystallographic characterization of Y_2C_{2n} (2n = 82, 88−94): direct Y−Y bonding and cage-dependent cluster evolution. *Chem. Sci.* **2019**, *10*, 4707−4713.
(31) Wu, X.; Lu, X. Dimetalloendofullerene U_2@C_{60} Has a U−U Multiple Bond Consisting of Sixfold One-Electron-Two-Center Bonds. *J. Am. Chem. Soc.* **2007**, *129*, 2171−2177.
(32) Infante, I.; Gagliardi, L.; Scuseria, G. E. Is Fullerene C_{60} Large Enough to Host a Multiply Bonded Dimetal? *J. Am. Chem. Soc.* **2008**, *130*, 7459−7465.
(33) Foroutan-Nejad, C.; Vícha, J.; Marek, R.; Patzschke, M.; Straka, M. Unwilling U−U bonding in U_2@C_{80}: cage-driven metal−metal bonds in di-uranium fullerenes. *Phys. Chem. Chem. Phys.* **2015**, *17*, 24182−24192.
(34) Pyykko, P.; Zhao, Y. The large range of uranyl bond lengths: ab initio calculations on simple uranium-oxygen clusters. *Inorg. Chem.* **1991**, *30*, 3787−3788.
(35) Atwood, J. L.; Koutsantonis, G. A.; Raston, C. L. Purification of C_{60} and C_{70} by selective complexation with calixarenes. *Nature* **1994**, *368*, 229−231.
(36) Zhang, D.; Ronson, T. K.; Nitschke, J. R. Functional Capsules via Subcomponent Self-Assembly. *Acc. Chem. Res.* **2018**, *51*, 2423−2436.
(37) Fuertes-Espinosa, C.; García-Simón, C.; Castro, E.; Costas, M.; Echegoyen, L.; Ribas, X. A Copper-based Supramolecular Nanocapsule that Enables Straightforward Purification of Sc_3N-based Endohedral Metallofullerene Soots. *Chem. - Eur. J.* **2017**, *23*, 3553−3557.
(38) Fuertes-Espinosa, C.; Gómez-Torres, A.; Morales-Martínez, R.; Rodríguez-Fortea, A.; García-Simón, C.; Gándara, F.; Imaz, I.; Juanhuix, J.; Maspoch, D.; Poblet, J. M.; Echegoyen, L.; Ribas, X. Purification of Uranium-based Endohedral Metallofullerenes (EMFs) by Selective Supramolecular Encapsulation and Release. *Angew. Chem., Int. Ed.* **2018**, *57*, 11294−11299.
(39) Zhang, J.; Bowles, F. L.; Bearden, D. W.; Ray, W. K.; Fuhrer, T.; Ye, Y.; Dixon, C.; Harich, K.; Helm, R. F.; Olmstead, M. M.; Balch, A. L.; Dorn, H. C. A missing link in the transformation from asymmetric to symmetric metallofullerene cages implies a top-down fullerene formation mechanism. *Nat. Chem.* **2013**, *5*, 880.
(40) Cai, W.; Li, F.-F.; Bao, L.; Xie, Y.; Lu, X. Isolation and Crystallographic Characterization of La_2C_2@C_s(574)-C_{102} and La_2C_2@C_2(816)-C_{104}: Evidence for the Top-Down Formation Mechanism of Fullerenes. *J. Am. Chem. Soc.* **2016**, *138*, 6670−6675.
(41) Bao, L.; Yu, P.; Pan, C.; Shen, W.; Lu, X. Crystallographic identification of Eu@C_{2n} (2n = 88, 86 and 84): completing a transformation map for existing metallofullerenes. *Chem. Sci.* **2019**, *10*, 2153.
(42) Curl, R. F.; Haddon, R. C. On the Formation of the Fullerenes and Discussion. *Philosophical Transactions of the Royal Society of London. Series A: Physical and Engineering Sciences* **1993**, *343*, 19−32.
(43) Dunk, P. W.; Mulet-Gas, M.; Nakanishi, Y.; Kaiser, N. K.; Rodríguez-Fortea, A.; Shinohara, H.; Poblet, J. M.; Marshall, A. G.; Kroto, H. W. Bottom-up formation of endohedral mono-metallofullerenes is directed by charge transfer. *Nat. Commun.* **2014**, *5*, 5844.
(44) Dunk, P. W.; Kaiser, N. K.; Hendrickson, C. L.; Quinn, J. P.; Ewels, C. P.; Nakanishi, Y.; Sasaki, T.; Shinohara, H.; Marshall, A. G.; Kroto, H. W. Closed network growth of fullerenes. *Nat. Commun.* **2012**, *3*, 855.
(45) Dunk, P. W.; Kaiser, N. K.; Mulet-Gas, M.; Rodríguez-Fortea, A.; Poblet, J. M.; Shinohara, H.; Hendrickson, C. L.; Marshall, A. G.; Kroto, H. W. The Smallest Stable Fullerene, M@C_{28} (M = Ti, Zr, U): Stabilization and Growth from Carbon Vapor. *J. Am. Chem. Soc.* **2012**, *134*, 9380−9389.
(46) Mulet-Gas, M.; Abella, L.; Dunk, P. W.; Rodríguez-Fortea, A.; Kroto, H. W.; Poblet, J. M. Small endohedral metallofullerenes: exploration of the structure and growth mechanism in the Ti@C_{2n} (2n = 26−50) family. *Chem. Sci.* **2015**, *6*, 675−686.
(47) Chen, C.-H.; Ghiassi, K. B.; Cerón, M. R.; Guerrero-Ayala, M. A.; Echegoyen, L.; Olmstead, M. M.; Balch, A. L. Beyond the Butterfly: Sc_2C_2@C_{2v}(9)-C_{86}, an Endohedral Fullerene Containing a

DOI: 10.1021/acs.accounts.9b00229
Acc. Chem. Res. 2019, 52, 1824−1833

Planar, Twisted Sc_2C_2 Unit with Remarkable Crystalline Order in an Unprecedented Carbon Cage. *J. Am. Chem. Soc.* **2015**, *137*, 10116−10119.
(48) Chen, C.-H.; Abella, L.; Cerón, M. R.; Guerrero-Ayala, M. A.; Rodríguez-Fortea, A.; Olmstead, M. M.; Powers, X. B.; Balch, A. L.; Poblet, J. M.; Echegoyen, L. Zigzag Sc_2C_2 Carbide Cluster inside a [88]Fullerene Cage with One Heptagon, $Sc_2C_2@C_s$(hept)-C_{88}: A Kinetically Trapped Fullerene Formed by C_2 Insertion? *J. Am. Chem. Soc.* **2016**, *138*, 13030−13037.
(49) Hernández, E.; Ordejón, P.; Terrones, H. Fullerene growth and the role of nonclassical isomers. *Phys. Rev. B: Condens. Matter Mater. Phys.* **2001**, *63*, 193403.
(50) Garcia-Borràs, M.; Cerón, M. R.; Osuna, S.; Izquierdo, M.; Luis, J. M.; Echegoyen, L.; Solà, M. The Regioselectivity of Bingel−Hirsch Cycloadditions on Isolated Pentagon Rule Endohedral Metallofullerenes. *Angew. Chem., Int. Ed.* **2016**, *55*, 2374−2377.
(51) Aroua, S.; Garcia-Borràs, M.; Bölter, M. F.; Osuna, S.; Yamakoshi, Y. Endohedral Metal-Induced Regioselective Formation of Bis-Prato Adduct of $Y_3N@I_h$-C_{80} and $Gd_3N@I_h$-C_{80}. *J. Am. Chem. Soc.* **2015**, *137*, 58−61.
(52) Cerón, M. R.; Izquierdo, M.; Garcia-Borràs, M.; Lee, S. S.; Stevenson, S.; Osuna, S.; Echegoyen, L. Bis-1,3-dipolar Cycloadditions on Endohedral Fullerenes $M_3N@I_h$-C_{80} (M = Sc, Lu): Remarkable Endohedral-Cluster Regiochemical Control. *J. Am. Chem. Soc.* **2015**, *137*, 11775−11782.
(53) Cerón, M. R.; Maffeis, V.; Stevenson, S.; Echegoyen, L. Endohedral fullerenes: Synthesis, isolation, mono- and bis-functionalization. *Inorg. Chim. Acta* **2017**, *468*, 16−27.

DOI: 10.1021/acs.accounts.9b00229
Acc. Chem. Res. 2019, 52, 1824−1833